



Contents lists available at ScienceDirect

Bioorganic & Medicinal Chemistry

journal homepage: www.elsevier.com/locate/bmc

Convergent ^{18}F -labeling and evaluation of *N*-benzylphenethylamines as 5-HT_{2A} receptor PET ligands

Ida Nymann Petersen^a, Jonas Villadsen^b, Hanne Demant Hansen^b, Anders A. Jensen^a, Szabolcs Lehel^c, Nic Gillings^c, Matthias M. Herth^{a,c}, Gitte M. Knudsen^b, Jesper L. Kristensen^{a,*}

^a Department of Drug Design and Pharmacology, Faculty of Health and Medical Sciences, University of Copenhagen, Universitetsparken 2, 2100 København Ø, Denmark

^b Center for Integrated Molecular Brain Imaging (CIMBI), Rigshospitalet and University of Copenhagen, Blegdamsvej 9, 2100 Copenhagen, Denmark

^c Department of Clinical Physiology, Nuclear Medicine and PET, Rigshospitalet, Blegdamsvej 9, 2100 Copenhagen, Denmark

ARTICLE INFO

Article history:

Received 30 June 2016

Revised 22 August 2016

Accepted 27 August 2016

Available online xxxxx

Keywords:

 ^{18}F -labeling

PET

Serotonin

5-HT_{2A} receptor agonist

ABSTRACT

Positron emission tomography (PET) investigations of the 5-HT_{2A} receptor (5-HT_{2A}R) system can be used as a research tool in diseases such as depression, Alzheimer's disease and schizophrenia. We have previously developed a ^{11}C -labeled agonist PET ligand (^{11}C]-Cimbi-36), and the aim of this study was to identify a ^{18}F -labeled analogue of this PET-ligand. Thus, we developed a convergent radiochemical approach giving easy access to 5 different ^{18}F -labeled ligands structurally related to Cimbi-36 from a common ^{18}F -labeled intermediate. After intravenous injection, all ligands entered the pig brain. However, since within-scan intervention with ketanserin, a known orthosteric 5-HT_{2A} receptor antagonist, did not result in significant blocking, the radioligands seem unsuitable for neuroimaging of the 5-HT_{2A}R in vivo.

© 2016 Elsevier Ltd. All rights reserved.

1. Introduction

The serotonin 2A receptor (5-HT_{2A}R) is involved in the regulation of several brain functions, such as appetite, emotion, body temperature and the sleep/wake cycle, and important for numerous diseases, for example depression, Alzheimer's and schizophrenia.^{1,2} Positron Emission Tomography (PET) imaging is a sensitive and non-invasive in vivo imaging tool. PET imaging can be used for diagnosis, therapy planning and monitoring,³ and 5-HT_{2A}R antagonist PET-ligands such as [^{18}F]-Altanserin and [^{11}C]-MDL-10097 are routinely used in a clinical setting.^{4–7} Recently, an effort has been made to expand the toolbox of PET ligands applicable for quantification of 5-HT_{2A}R levels in the human brain. Antagonist radioligands bind to the global population of receptors, whereas an agonist radioligand should be able to image only the population of functional receptors, i.e., those mediating neurotransmitter signaling.^{8,9}

To address this shortcoming of the available PET-ligands in the 5-HT_{2A}R field, we have previously developed an agonist PET-ligand, [^{11}C]-Cimbi-36, for this receptor.^{10,11} Herein, we detail some of our efforts towards the development of a ^{18}F -labeled version of

Cimbi-36. ^{18}F has several advantages compared to ^{11}C for PET studies: the isotope has a longer physical half-life, it can produce images with higher resolution, and it is possible to transport ^{18}F -labeled radioligands to other facilities. Towards that goal, we recently reported an attempt to develop a ^{18}F -labeled version of [^{11}C]-Cimbi-36 via substitution of all three possible methoxy groups with a [^{18}F]-FCH₂CH₂O-group.¹² Unfortunately, these ligands were unable to penetrate the blood brain barrier to any major extent.

In the present study, we introduced a ^{18}F at another position in the Cimbi-36 molecule hoping that this structural modification neither would be detrimental to the compounds ability to enter the brain nor to its binding affinity to the 5-HT_{2A}R. The position of the fluorine was also selected to allow us to introduce ^{18}F in a convergent manner from a common ^{18}F -labeled intermediate. In the development of [^{11}C]-Cimbi-36 we observed that subtle modifications to the 4-position in the molecule had dramatic effects on brain uptake and PET-ligand kinetics¹⁰ as well as their pharmacological profile.¹³ Therefore we wanted to be able to screen ligands with various 4-substituents and targeted the ligands shown in **Figure 1**. Halogenated analogues **2–4** were selected as direct analogues of previously screened ^{11}C -labeled analogues of Cimbi-36 possessing the best overall profiles with respect to affinity for 5-HT_{2A}R and ability to cross the blood–brain-barrier, whereas **5** and **6** were included as the introduction of the NO₂ and CN groups with their different physicochemical characteristics was expected to

* Corresponding author. Tel.: +45 35336487.

E-mail address: jesper.kristensen@sund.ku.dk (J.L. Kristensen).

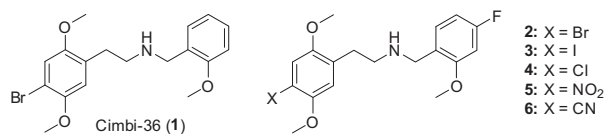


Figure 1. Structure of Cimbi-36 (**1**) and targeted derivatives amenable for ^{18}F -labeling (**2–6**).

exert more pronounced effects on the behavior of the prospective PET ligands.

2. Results and discussion

Compounds **2–6** were synthesized via reductive amination with 4-fluoro-2-methoxybenzaldehyde and the appropriately substituted phenethylamines, see [Supporting information](#) for details.

The binding affinities of the six ligands at the human 5-HT_{2A} ($h5\text{-HT}_{2A}$) and 5-HT_{2C} ($h5\text{-HT}_{2C}$) receptors were determined using membranes from tsA201 cells transiently expressing the two receptors in a [^3H]Cimbi-36 competition binding assay as previously described.¹²

The addition of a fluorine onto Cimbi-36 (**1**) to give **2** decreased the binding affinities to both $h5\text{-HT}_{2A}\text{R}$ and $h5\text{-HT}_{2C}\text{R}$ with ~ 16 -fold, and thus the 2A/2C selectivity ratio of **2** was similar to that of **1** ([Table 1](#)). Substitution of the bromine in **2** with an iodine yielded an analog **3** with slightly improved binding affinities to both $h5\text{-HT}_{2A}\text{R}$ and $h5\text{-HT}_{2C}\text{R}$, although these binding affinities were ~ 7 -lower than those exhibited by Cimbi-36 at the two receptors ([Table 1](#)). The binding affinities exhibited by chloro-analog **4** at the two receptors were further reduced compared to **2** and **3**. Finally, the introduction of a NO_2 or a CN group in this position resulted in analogs displaying substantially reduced binding affinities at the receptors. Interestingly, although analog **6** displayed a ~ 500 fold lower binding affinity at $h5\text{-HT}_{2A}\text{R}$ than **1**, the reduction in $h5\text{-HT}_{2C}\text{R}$ binding affinity for this analog was considerably larger, resulting in **6** exhibiting pronounced binding selectivity for $5\text{-HT}_{2A}\text{R}$ over $5\text{-HT}_{2C}\text{R}$. A broad screen of analog **2** at the NIMH Psychoactive Drug Screening Program¹⁴ (PDSP) showed that the compound is at least two orders of magnitude selective towards 5-HT_{2A}

and 5-HT_{2C} compared with a range of different CNS targets—as is the case for **1**, see [Supporting information](#) for details.

The functional properties of **2** at the $h5\text{-HT}_{2A}$ and the $h5\text{-HT}_{2C}$ receptors were determined at HEK293 cell lines stably expressing the two receptors in a fluorescence-based Ca^{2+} imaging assay using Fluo-4 as dye ([Table 2](#)).¹⁵ In good agreement with their $5\text{-HT}_{2A}\text{R}$ binding affinities, **2** exhibited 7-fold lower agonist potency at the receptor than **1**, and its potency at $5\text{-HT}_{2C}\text{R}$ was even lower (100-fold) compared to that of **1**, and thus **2** exhibited 15-fold functional selectivity between the receptors in this assay. Interestingly, the introduction of the fluorine into **1** converted it from a full agonist into a partial agonist at $5\text{-HT}_{2C}\text{R}$, whereas the intrinsic activities of **1** and **2** as $5\text{-HT}_{2A}\text{R}$ agonists were comparable.

All in all, these data suggested that the introduction of a fluorine into this position of Cimbi-36 is tolerated, and based on their respective in vitro binding properties we proceeded to develop a radiochemical route to ^{18}F -labeled versions of analogs **2–6**.

We previously investigated the one-pot ^{11}C -labeling of benzaldehydes and subsequent reductive amination with 4-substituted phenethylamines to produce ^{11}C -labeled PET-ligands from the Cimbi-36 structural class.¹⁶ Using this approach a series of ^{11}C -labeled compounds was produced from the same radiolabeled intermediate. This greatly simplifies the screening of new PET-ligands, as precursor synthesis and radiochemical development can be reduced to a minimum. In the current study we wanted to develop a similar setup where the ^{18}F -labeling of an aldehyde and subsequent reductive amination could be performed in a one-pot reaction. ^{18}F can generally be introduced on electron deficient aromatic rings via nucleophilic substitution of a leaving group such as halogens, a NO_2 -group, or ideally a trimethyl ammonium salt. The synthesis of aldehyde [^{18}F]**9** (see [Scheme 1](#)) has previously been reported from the corresponding NO_2 -precursor,^{17,18} but since excess of the aldehyde would react with the phenethylamine and give products with similar polarity as the desired PET-ligands, this procedure could complicate the final purification of the PET-ligands. Thus, we decided to target the trimethylammonium salt **8** as precursor instead as it generally gives better incorporation yields and the polarity of the trimethylammonium reagent is very different from the final PET-ligands due to the fixed

Table 1
Binding affinities of **1–6** at $h5\text{-HT}_{2A}\text{R}$ and $h5\text{-HT}_{2C}\text{R}$

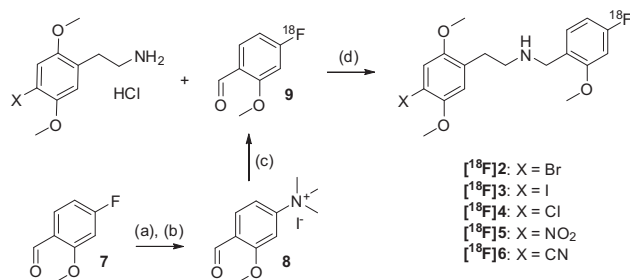
	$h5\text{-HT}_{2A}\text{R}$	$h5\text{-HT}_{2C}\text{R}$	K_i^{2C}/K_i^{2A}
1	0.21 [9.68 \pm 0.09] (8)	2.5 [8.60 \pm 0.07] (6)	12
2	3.3 [8.48 \pm 0.03] (3)	39 [7.41 \pm 0.06] (4)	12
3	1.5 [8.82 \pm 0.08] (4)	18 [7.74 \pm 0.08] (3)	12
4	7.7 [8.11 \pm 0.03] (4)	67 [7.18 \pm 0.06] (3)	8
5	30 [7.53 \pm 0.03] (3)	250 [6.60 \pm 0.08] (4)	8
6	120 [6.93 \pm 0.14] (3)	$\sim 10,000$ [~ 5.0] (3)	~ 85

The affinities were determined in a competition assay using [^3H]Cimbi-36 (**1**) as radio ligand and membranes from tsA201 cells transiently expressing human 5-HT_{2A} and 5-HT_{2C} receptors. The K_i values for the analogs are given in nM with $pK_i \pm \text{SEM}$ values in brackets. The number of experiments (n) is given in parenthesis after each value.

Table 2
Functional properties of **1** and **2** at $h5\text{-HT}_{2A}\text{R}$ and $h5\text{-HT}_{2C}\text{R}$

	EC_{50} [$p\text{EC}_{50} \pm \text{SEM}$]		$R_{\text{max}}(\%) \pm \text{SEM}$	
	$h5\text{-HT}_{2A}\text{R}$	$h5\text{-HT}_{2C}\text{R}$	$h5\text{-HT}_{2A}\text{R}$	$h5\text{-HT}_{2C}\text{R}$
1	9.02 \pm 0.09	9.04 \pm 0.06	83 \pm 3	99 \pm 7
2	8.17 \pm 0.08	7.00 \pm 0.05	75 \pm 6	52 \pm 4

Stable $h5\text{-HT}_{2A}$ - and $h5\text{-HT}_{2C}$ -HEK293 cell lines were used in the Ca^{2+} /Fluo-4/assay. The EC_{50} values (given in nM with $p\text{EC}_{50} \pm \text{SEM}$ values) and $R_{\text{max}} \pm \text{SEM}$ values (given in % of the maximal response evoked by 5-HT at the receptor) are based on 3 independent experiments.



Scheme 1. Convergent ^{18}F -labeling of **2–6**. Reaction and conditions: (a) Me_2NH , DMF, 75 °C, 86% (b) MeI, 7 days, 22% (c) [^{18}F]/FK, K_{222} , DMSO, 70 °C (d) NaBCNH_3 , AcOH, DMSO, 130 °C.

positive charge. The synthesis of the aldehyde precursor; 4-formyl-3-methoxy-*N,N,N*-trimethylbenzenaminium iodide was accomplished in two steps: addition of dimethylamine to **7** gave 4-(dimethylamino)-2-methoxybenzaldehyde in 86% yield which subsequently was quaternized by stirring it in neat MeI for a week at room temperature. This caused the desired trimethylammonium precursor **8** to precipitate which was isolated by filtration in 22% yield. Attempts to shorten the reaction time by heating of the reaction mixture caused decomposition.

The labeling of the aldehyde was performed in DMSO at 70 °C for 10 min giving consistent high incorporation yields (between 75% and 90%) as determined by TLC and HPLC analysis. In comparison, it is necessary to heat the corresponding NO₂-precursor to 140 °C in order to obtain similar yields of [¹⁸F]**9**.¹⁸ With the required ¹⁸F-labeled aldehyde in hand we set out to identify conditions that would allow us to couple it with the selected phenethylamines. Initially the condition used for the reductive amination of the ¹¹C-labeled aldehydes and similar procedures reported earlier^{16,19} were investigated but this led to poor yields of the desired radioligands. Thus, several parameters were optimized, and it was found that increasing the amount of K₂CO₃ and K₂S₂O₈ in the first step (in an attempt to reduce the amount of ¹⁸F sticking to the reaction vial), increasing the reaction time and changing the solvent to DMSO improved the radiochemical yield—but problems with reproducibility persisted. Careful scrutiny of several parameters revealed that the quality of the NaCNBH₃ used in the reduction of the imine is of crucial importance for the success of the reaction. Purification of NaCNBH₃ as previously described²⁰ and storing/handling it under dry conditions at all times led to consistently higher radiochemical yields. With these conditions we were able to produce 1.5–7 GBq of the final product in less than 1 h from a 10 min irradiation in a fully automated radiosynthesis system.

The pigs were scanned with a high resolution research tomography (HRRT) scanner (Siemens AG). The ¹⁸F-labeled radio ligands exhibited good brain uptake and reversible binding, see Figure 2. The highest uptake was observed in thalamus, followed by high neocortical uptake, moderate striatal and low cerebellar uptake, except for the high thalamus uptake this distribution is in accordance with the known 5-HT_{2A}R distribution in the pig brain.^{6,10} We speculate that the thalamic uptake is due to off-target binding to a target not included in the broad PDSP-screening of **2**. [¹⁸F]**6** shows very high uptake in bone tissue, and by the end of the scan the great majority of activity stems from the skull. This could be a result of defluorination of the PET-ligand, as bone tissue is known to take up fluoride ions.²¹ Thus, it is possible that cortical uptake in the later frames of the scan is overestimated due to spill-over of radioactivity from the skull.

When attempting to displace the ¹⁸F-labeled radioligands from the 5-HT_{2A}R with a within-scan challenge with the known orthosteric 5-HT_{2A}R antagonist ketanserin, we did not see any significant decrease in binding for any of the radioligands. Apart from [¹⁸F]**3**, injection of ketanserin was followed by an increase in plasma radioactivity. This likely represents displacement of the radioligand from peripheral 5-HT_{2A}R sites into blood, which then leads to an increased input to the brain. This confirms that the ligands exhibit specific 5-HT_{2A}R binding in vivo, and thus we speculate that the lack of displacement in the brain could be due to the majority of the radioactivity in the brain representing off-target binding. Lack of displacement could also be caused by a self-blocking effect, i.e., not fulfilling the tracer principle of only having a occupancy of 5–10% with the PET-ligand itself. The specific activities of the ¹⁸F-labeled ligands were between 9 and 177 GBq/μmol.

To assess whether low specific activity was the reason for the observed lack of displacement, we decided to evaluate [¹¹C]**2**

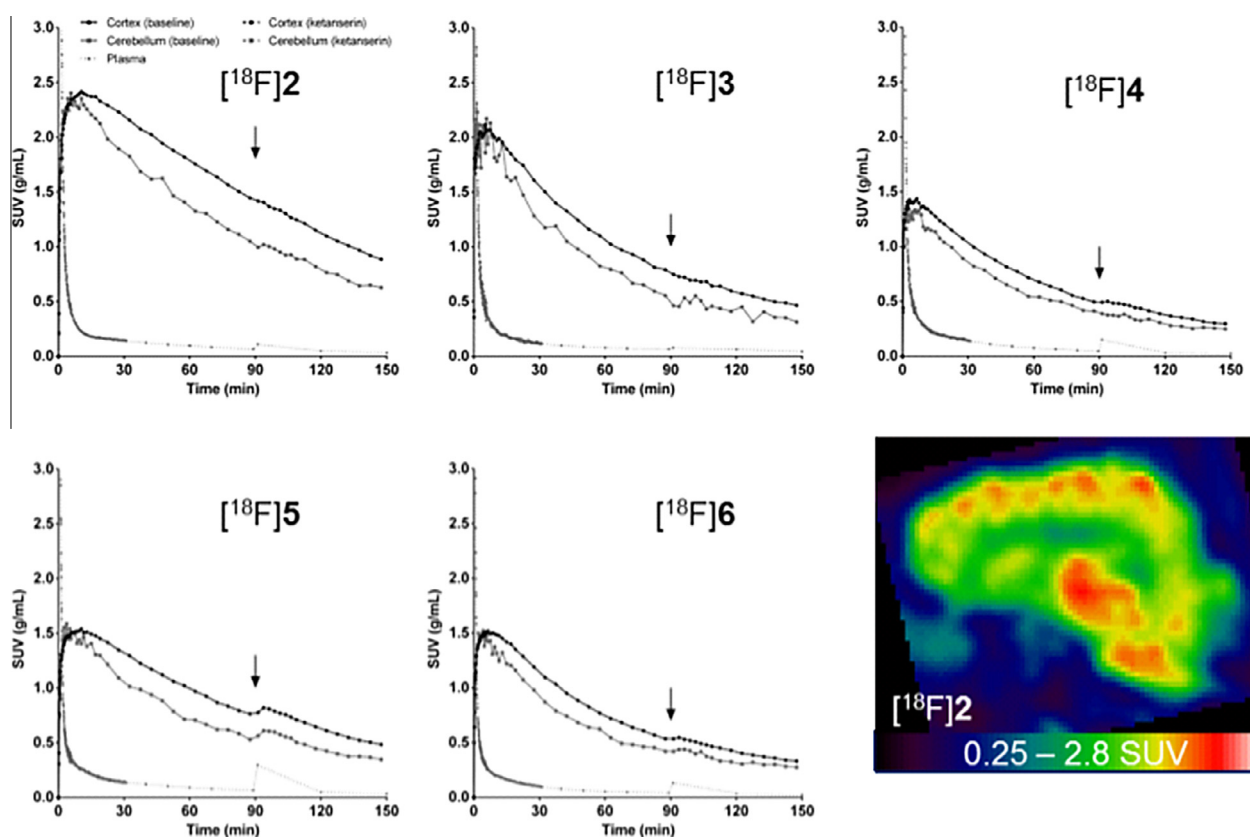


Figure 2. Time activity curves (TACs) from PET-experiments in pigs with overlay of metabolite-corrected plasma radioactivity for the [¹⁸F]**2**–**6** in cortex, cerebellum and plasma. The arrows represent the time points for the administration of a ketanserin challenge. The sagittal image shows the distribution of [¹⁸F]**2** in the pig brain.

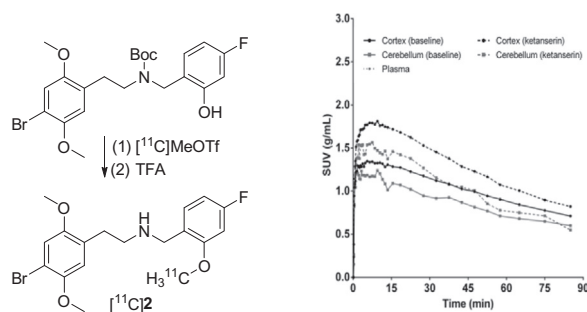


Figure 3. Radiosynthesis of $[^{11}\text{C}]\mathbf{2}$ and TACs with overlay of metabolite-corrected plasma radioactivity for $[^{11}\text{C}]\mathbf{2}$ in cortex and cerebellum. The dotted lines represent a separate experiment in which a blocking dose of ketanserin (3 mg/kg + 1 mg/kg/h) was administered prior $[^{11}\text{C}]\mathbf{2}$.

thereby ensuring high specific activity (≥ 500 GBq/ μmol). The ^{11}C -labeling was performed in analogy to the labeling of $[^{11}\text{C}]\mathbf{1}$ from the corresponding precursor, see Figure 3.

In vivo evaluation of $[^{11}\text{C}]\mathbf{2}$ in a pig confirmed the data from the experiments with $[^{18}\text{F}]\mathbf{2}$; the binding in the cortical areas could not be blocked by pretreatment with ketanserin. Quantifying the binding of $[^{11}\text{C}]\mathbf{2}$ with full arterial input modeling (data not shown) revealed no decrease in distribution volumes across the investigated regions. The observed increased uptake and distribution volume of the block scan with $[^{11}\text{C}]\mathbf{2}$, as well as the slight increase in binding for $[^{18}\text{F}]\mathbf{5}$ and $[^{18}\text{F}]\mathbf{6}$ after ketanserin administration, is thus interpreted as displacement of radioligand from peripheral 5-HT_{2A}R sites leading to increase in radioligand concentration in the blood and brain compartments. This leads us to conclude that neither low specific activity nor the within-scan challenge approach seems to be the reason to the lack of displacement. Thus, decorating the Cimbi-36 scaffold with a single fluorine in the selected position (going from **1** to **2**) renders the ligands unsuitable for in vivo imaging of the 5-HT_{2A}R.

3. Conclusion

We successfully ^{18}F -labeled five new 5-HT_{2A}R agonist radioligands from a common ^{18}F -labeled benzaldehyde intermediate. The radio synthesis of this previously reported benzaldehyde was optimized using a trimethylammonium precursor, with the following improvements: The introduction of ^{18}F can be performed at lower temperature due to the higher reactivity of the precursor and the final purification is facilitated by the presence of a fixed positive charged in the precursor—simplifying chromatographic purification. Medium to high brain uptake of these ^{18}F -labeled ligands was seen in pigs, but none of the tested radioligands could be displaced by ketanserin indicating that they are not suitable for neuroimaging of the 5-HT_{2A}R.

Acknowledgments

The authors thank the Lundbeck Foundation and the Novo Nordisk Foundation for funding and the technical staff at the PET and cyclotron unit for assistance.

A. Supplementary data

Supplementary data (full experimental detail, description of the assays, radiochemistry and animal procedures) associated with this article can be found, in the online version, at <http://dx.doi.org/10.1016/j.bmc.2016.08.056>.

References and notes

- Gonzalez-Maeso, J.; Sealfon, S. C. *Trends Neurosci.* **2009**, *32*, 225.
- Popa, D.; Léna, C.; Fabre, V.; Prenat, C.; Gingrich, J.; Escourrou, P.; Hamon, M.; Adrien, J. *J. Neurosci.* **2005**, *25*, 11231.
- Piel, M.; Vernaleken, I.; Rösch, F. *J. Med. Chem.* **2014**, *57*, 9232.
- Lemaire, C.; Cantineau, R.; Guillaume, M.; Plenevaux, A.; Christiaens, L. *J. Nucl. Med.* **1991**, *32*, 2266.
- Paterson, L. M.; Kornum, B. R.; Nutt, D. J.; Pike, V. W.; Knudsen, G. M. *Med. Res. Rev.* **2013**, *33*, 54.
- Hansen, H.; Herth, M. M.; Ettrup, A.; Dyssegaard, A.; Knudsen, G. M. *J. Labeled. Compd. Rad.* **2013**, *56*, 338.
- Debus, F.; Herth, M. M.; Piel, M.; Buchholz, H. G.; Bausbacher, N.; Kramer, V.; Lüddens, H.; Rösch, F. *Nucl. Med. Biol.* **2010**, *37*, 487.
- Paterson, L. M.; Tyacke, R. J.; Nutt, D. J.; Knudsen, G. M. *JCBFM* **2010**, *30*, 1682.
- Narendran, R.; Mason, N. S.; Laymon, C. M.; Lopresti, B. J.; Velasquez, N. D.; May, M. A.; Kendro, S.; Martinez, D.; Mathis, C. A.; Frankle, W. G. *J. Pharmacol. Exp. Ther.* **2010**, *333*, 533.
- Ettrup, A.; Hansen, M.; Santini, M. A.; Paine, J.; Gillings, N.; Palner, M.; Lehel, S.; Herth, M. M.; Madsen, J.; Kristensen, J. L.; Begtrup, M.; Knudsen, G. M. *Eur. J. Nucl. Med. Mol.* **2010**, *38*, 681.
- Ettrup, A.; Cunha-Bang, S.; McMahon, B.; Lehel, S.; Dyssegaard, A.; Skibsted, A. W.; Jørgensen, L. M.; Hansen, M.; Baandrup, A. O.; Bache, S.; Svarer, C.; Kristensen, J. L.; Gillings, N.; Madsen, J.; Knudsen, G. M. *JCBFM* **2014**, *34*, 1188.
- Herth, M. M.; Petersen, I. N.; Hansen, H. D.; Hansen, M.; Ettrup, A.; Jensen, A. A.; Lehel, S.; Dyssegaard, A.; Gillings, N.; Knudsen, G. M.; Kristensen, J. L. *Nucl. Med. Bio.* **2016**, *43*, 455.
- Hansen, M.; Phonekeo, K.; Paine, J. S.; Leth-Petersen, S.; Begtrup, M.; Bräuner-Osborne, H.; Kristensen, J. L. *ACS Chem. Neurosci.* **2014**, *5*, 243.
- Besnard, J.; Ruda, G. F.; Setola, V.; Abecassis, K.; Rodriguiz, R. M.; Huang, X.-P.; Norval, S.; Sassano, M. F.; Shin, A. I.; Webster, L. A.; Simeons, F. R. C.; Stojanovski, L.; Prat, A.; Seidah, N. G.; Constam, D. B.; Bickerton, G. R.; Read, K. D.; Wetsel, W. C.; Gilbert, I. H.; Roth, B. L.; Hopkins, A. L. *Nature* **2012**, *492*, 215.
- Jensen, A. A.; Plath, N.; Pedersen, M. H. F.; Isberg, V.; Krall, J.; Wellendorph, P.; Stensbøl, T. B.; Gloriam, D. E.; Krogsgaard-Larsen, P.; Frølund, B. *J. Med. Chem.* **2013**, *56*, 1211.
- Herth, M. M.; Leth-Petersen, S.; Lehel, S.; Hansen, M.; Knudsen, G. M.; Gillings, N.; Madsen, J.; Kristensen, J. L. *Rsc. Adv.* **2014**, *4*, 21347.
- Shen, B.; Löffler, D.; Zeller, K.-P.; Übele, M.; Reischl, G.; Machulla, H.-J. *J. Fluor. Chem.* **2007**, *128*, 1461.
- Lemaire, C.; Libert, L.; Plenevaux, A.; Aerts, J.; Franci, X.; Luxen, A. *J. Fluor. Chem.* **2012**, *138*, 48.
- Hai-Bin, T.; Duan-Zhi, Y.; Jun-Ling, L.; Lan, Z.; Cun-Fu, Z.; Yong-Xian, W.; Wei, Z. *Radiochim Acta* **2003**, *91*, 241.
- Lane, C. F. *Synthesis-Stuttgart* **1975**, 135.
- Tipre, D. N.; Zoghbi, S. S.; Liow, J.-S.; Green, M. V.; Seidel, J.; Ichise, M.; Innis, R. B.; Pike, V. W. *J. Nucl. Med.* **2006**, *47*, 345.